JOURNAL OF SOLID STATE CHEMISTRY 112, 418–423 (1994)

The Praseodymium Hydrogenselenite $Pr_2(HSeO_3)_2(SeO_3)_2$: Synthesis, Characterization, and Crystal Structure

A. Castro,*,[1] R. Enjalbert,† M. de Pedro,* and J. C. Trombe†

*Instituto de Ciencia de Materiales de Madrid, CSIC, Serrano 113, 28006 Madrid, Spain; and †Centre d'Elaboration de Matériaux et d'Etudes Structurales, CNRS, 29 rue Jeanne Marvig, B.P. 4347, 31055 Toulouse Cedex, France

Received October 12, 1993; in revised form January 4, 1994; accepted January 5, 1994

Crystal growth of praseodymium hydrogenselenite $Pr_2(HSeO_3)_2(SeO_3)_2$ has been carried out by pseudohydrothermal synthesis. Its thermal decomposition gives rise to three new anhydrous rare-earth selenites, two of them isolated as tiny single crystals ($Pr_2Se_4O_{11}$ and $Pr_2Se_3O_9$). The structure of $Pr_2(HSeO_3)_2(SeO_3)_2$ has been solved in the orthorhombic symmetry, space group $Pbc2_1$, with unit-cell parameters $a = 7.0471(8)$, $b = 8.3480(8)$, and $c = 18.987(3)$ Å, and refined down to $R = 0.040$ and $R_w = 0.047$. Two crystallographically independent types of Pr atoms were found, coordinated to 10 O, giving rise to a tetradecahedron or *cis*-bicappped cube. The four present Se atoms are coordinated at 3 O (Se1 and Se4) or at one OH and 2 O (Se2 and Se3), in the classical form of a trigonal pyramid. Each Se1 and Se4 are linked to five praseodymium atoms, two bidentate and three monodentate bonding, while each Se2 and Se3 only bond one time bidentately and monodentately with Pr2 and Pr1, respectively. The structure can be described as a layered one, the sheets containing all the praseodymium and selenite groups are interconnected by hydrogen selenite groups, via hydrogen bonding. This material was also characterized by IR spectroscopy and magnetic measurements. © 1994 Academic Press, Inc.

INTRODUCTION

Mixed oxocompounds containing semimetallic *p*-elements in a low oxidation state, for instance, As(III), Sb(III), Se(IV), or Te(IV), have been largely investigated and exhibit a crystal chemistry characterized by their stereochemically active long pair of electrons (1–4). A particularly exciting case is the family of rare-earth selenites, due to the potential interest in their optical and magnetic properties. In fact, in the past years, a number of compounds with varied and interesting structures have been prepared and studied. These compounds have been described as having a layered structure, with groups of hydrogenselenite, selenite, and diselenite, such as $LaHSe_2O_6$ (5), $PrH_3(SeO_3)_2$ (Se_2O_5) (6), or hydrated $RH(SeO_3)_2 \cdot 2.5H_2O$ (7).

In this way, the authors have solved the crystal structure of the new hydrated neodymium hydrogenselenite $Nd(HSeO_3)(SeO_3) \cdot 2H_2O$ (8), which contains free water molecules occupying channels developed between layers. They have also made an effort to obtain and characterize, for the first time, anhydrous rare-earth selenites, with the general formula $R_2Se_4O_{11}$, $R_4Se_7O_{20}$, $R_2Se_3O_9$, or R_2SeO_5 (9, 10), as well as to determine the crystal structure of $Eu_2Se_5O_{13}$ (11).

This paper reports the synthesis, by pseudohydrothermal methods, of the new praseodymium hydrogenselenite $Pr_2(HSeO_3)_2(SeO_3)_2$, as well as its characterization by thermal analysis, IR spectroscopy, and magnetic measurements. The crystal structure, solved by X-ray single-crystal methods, is isostructural with the $LaHSe_2O_6$ compound (5). Although the Pr ionic radius is smaller than that of La, the Pr coordination number is 10. The existence of simultaneously double-edge- and single-corner-sharing selenite groups with praseodymium polyhedra, as well as the hydrogen bonding between the present sheets (H atoms localized), is emphasized.

EXPERIMENTAL

Synthesis

Crystal growth of the praseodymium selenite $Pr_2(HSeO_3)_2(SeO_3)_2$ has been carried out by pseudohydrothermal synthesis taking glass as precursor. The glass was obtained by heating a mixture of SeO_2 and Pr_2O_3 oxides (molar ratio, 12 : 1) for 36 hr at 460°C in a sealed evacuated Pyrex ampoule and followed by quenching in liquid N_2. Half a gram of this glass, together with 15 ml of water, was introduced into a covered Teflon cup (25 ml total volume), placed in a tightly closed steel container, and maintained at 120°C for a week; slow cooling was then applied (10°C/min). The light-green crystals obtained were washed with water and dried in air.

---

[1] To whom correspondence should be addressed.

0022-4596/94 $6.00

Characterization

Thermogravimetric and differential thermal analysis were performed in static air, at ambient pressure, between 25 and 1250°C, on a Stanton Redcroft STA-781 instrument, at a heating rate of 5°/min, and with an initial weight of about 10 mg. Standard platinum crucibles were used, alumina being the reference material. The IR spectrum (KBr pellets) was obtained on a FTIR 1725X Perkin–Elmer spectrometer. Magnetic measurements were carried out on a Quantum Design Squid susceptometer.

Crystal Structure Determination

The collection of the diffraction data was performed using an Enraf-Nonius CAD4 diffractometer. Orientation matrix and cell parameters were obtained from least-squares refinements of setting angles of 25 reflections. Table 1 summarizes physical and crystallographic data together with the experimental conditions of data collection. Corrections of Lorentz polarization and absorption (12) were applied to *h k l* data. Atomic scattering factors were corrected for anomalous dispersion (13). The calculations were performed with crystal (14) and drawings with ORTEP (15) run on a superminicomputer VFX/80 Aliant.

The structure was determined by the Patterson method, and the refinements were carried out by full-matrix least-squares calculations. The existence of hydrogen atoms, belonging to the $HSeO_3$ groups, was revealed by difference Fourier synthesis. The hydrogen atoms were introduced as fixed contributors. The absolute configuration did not yield significant results. In the final stage, each reflection was assigned a weight $w = 1/\sum_1^n A_n T_n(X)$, where n is the number of coefficients A for a Chebyschev series, T is the polynomial function, and X is $|F_o|/|F_o\max|$. Three coefficients A were used with the respective values 4.42, −2.39, and 3.27 (14). At that stage the largest (variable shift)/(e.s.d.) ratio was 0.01, and the final difference Fourier map did not give significant features.

TABLE 1

Experimental Crystallographic Data for $Pr_2(HSeO_3)_2(SeO_3)_2$

Crystal data	
Crystal system	orthorhombic
a	7.0471(8) Å
b	8.3480(8) Å
c	18.987(3) Å
V	1117(2) Å^3
Molecular weight	791.7
Morphology	platelet
Dimensions	0.37 × 0.12 × 0.02 mm
Transmission coefficient	0.86–4.36
Space group	$Pbc2_1$
Z	4
ρ_{cal}	4.71 g/cm^3
μ (Mo$K\alpha$)	215.6 cm^{-1}
$F(000)$	1404
Color	light green
Data collection	
Temperature	293 K
Wavelength (Mo$K\alpha$)	0.71073
Monochromator	Graphite
Scan mode	ω-2θ
Scan width	$(\Delta = 0.90 + 0.35 \tan \theta)°$
Take-off angle	3°
Maximum Bragg angle	30°
Scan speed	
SIGPRE	0.80
SIGMA	0.018
VPRE	10°/min
T_{max}	80 sec
Intensity control reflections	200/123/141 (every 3600 sec)
Orientation control reflections	600/0014/081 (every 100 reflections)
Indices range	$h = 0$–6, $k = 0$–8, $l = 0$–18
Structure refinement	
Reflections collected	2076
Reflections unique used	1309 ($I > 3\sigma(I)$)
Number of refined parameters	103
$R = \Sigma\lvert\lvert F_o\rvert - \lvert F_c\rvert\rvert/\Sigma\lvert F_o\rvert$	$R = 0.040$
$R_w = [\Sigma\, w(\lvert F_o\rvert - \lvert F_c\rvert)^2/\Sigma\, w F_o^2]^{1/2}$	$R = 0.047$

RESULTS AND DISCUSSION

Thermal Behavior

Thermal decomposition of $Pr_2(HSeO_3)_2(SeO_3)_2$ occur in four steps, between 100 and 1200°C, corresponding to the successive losses of H_2O and SeO_2 (Fig. 1). The first process starts at 275°C and is complete at 350°C. It corresponds to the loss of one molecule of water, leading to an unknown anhydrous praseodymium selenite, $Pr_2Se_4O_{11}$. The seond process, from 370 to 555°C, is attributed to the further degradation of this phase with the elimination of one molecule of SeO_2, giving rise to other anhydrous praseodymium selenite of composition $Pr_2Se_3O_9$, whose thermal behavior has been described elsewhere (9).

The DTA curve shows three endothermic peaks, in accordance with the three first mass losses, and one exothermic process due to the elimination of the last SeO_2 molecule, to obtain Pr_2O_3, and the simultaneous partial oxidation of it, giving rise to the more stable praseodymium oxide, Pr_6O_{11}.

When the heating and cooling rate of these decomposition processes is carried out very slowly, the two first anhydrous praseodymium selenites, $Pr_2Se_4O_{11}$ and $Pr_2Se_3O_9$, can be isolated as tiny single crystals, while the last one, Pr_2SeO_5, is always obtained as microcrystalline powder.

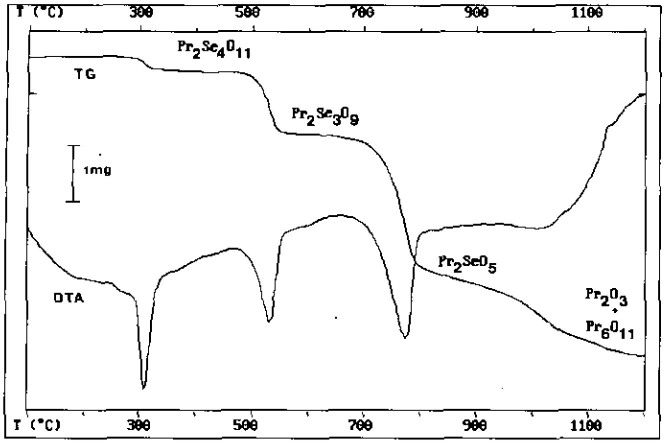

FIG. 1. TG and DTA curves of $Pr_2(HSeO_3)_2(SeO_3)_2$.

Infrared Spectrum and Magnetic Measurements

The IR spectrum of $Pr_2(HSeO_3)_2(SeO_3)_2$ permits the verification of the existence of SeO_3^{2-} and $HSeO_3^-$ groups. In fact, this spectrum exhibits the classical vibrations between 440 and 840 cm^{-1}, attributed to the selenite anion, as well as another band at 1265 cm^{-1}, ascribed to the hydrogenselenite anion (16, 17).

On the other hand, magnetic measurements of this compound have been carried out in order to confirm the valence of praseodymium cations. While the expected theoretical value is 3.58 μ_B for one Pr(III), the mean experimental value is 3.48 μ_B, which confirms the 3+ oxidation state of the praseodymium and may involve a possible interaction between neighboring cations.

Description of the Structure

The final list of fractional coordinates and equivalent isotropic thermal parameters are given in Table 2, and Table 3 lists selected bond distances and angles.

In the unit cell there are two crystallographically independent praseodymium and four selenium atoms. All the oxygen are related with selenium atoms (O1, O2, and O3 belong to the Se1 atoms, . . .), and O6 and O7 belong to the hydroxyl groups. Both Pr are coordinated to 10 oxygen atoms (with the exception of the hydroxyl groups) occupying the corners of distorted tetradecahedra or *cis*-bicapped cubes. For instance, Fig. 2 represents the coordination polyhedron of Pr2, where it can be seen that the praseodymium atom is situated in a cube whose corners are O1, O4, $O10^c$, $O12^c$, $O2^e$, $O4^f$, O5, and O11, the capping atoms being $O3^f$ and O12. The Pr–O distances vary from 2.47 to 2.77 Å, with an average of 2.58 Å for both Pr1 and Pr2 (Table 3). The praseodymium polyhedra are linked together, sharing edges of equivalent praseodymium atoms along the [010] direction, Pr1–O2O8–Pr1 . . . and Pr2–O4O12–Pr2 . . . , leading to chains at $x \approx 0$ and $x \approx 1/2$, respectively (Fig. 3). These chains are interconnected with the two of its neighbor's by sharing triangular faces, . . . Pr1–O1O10^{c}O12–Pr2–O2^{e}O3^f O11–Pr1^e . . . , along the [100] axis, making up infinitely dense layers parallel to the (001) plane, at the levels $z \approx 0$ and $z \approx 1/2$. Each Pr atom is surrounded by five other

TABLE 2

Final Least-Squares Atomic Parameters with Estimated Standard Deviations for $Pr_2(HSeO_3)_2(SeO_3)_2$

Atom	x	y	z	B_{eq} (Å^2) or B_{iso}
Pr1[a]	0.0819(1)	0.15682(9)	0	0.72(3)
Pr2[a]	0.5835(3)	0.05301(9)	−0.08724(6)	0.71(3)
Se1[a]	0.0709(3)	−0.0937(2)	−0.1410(1)	0.69(5)
Se2[a]	0.5792(3)	−0.1724(2)	−0.2387(1)	1.16(6)
Se3[a]	0.0633(3)	0.3756(2)	0.1479(1)	1.30(6)
Se4[a]	0.5659(2)	0.3074(2)	0.0512(1)	0.63(5)
O1	0.235(2)	0.032(2)	−0.1048(7)	1.4(2)
O2	−0.099(2)	−0.076(1)	−0.0725(6)	1.0(2)
O3	0.140(2)	−0.277(2)	−0.1166(8)	1.4(2)
O4	0.516(2)	−0.210(1)	−0.1557(7)	1.0(2)
O5	0.684(2)	0.005(2)	−0.2218(7)	1.8(2)
O6	0.371(3)	−0.088(2)	−0.2725(9)	2.7(3)
O7	−0.173(2)	0.335(2)	−0.1782(8)	1.4(2)
O8	0.028(2)	0.419(1)	0.0655(6)	0.7(2)
O9	0.141(2)	0.189(2)	0.1385(8)	1.7(2)
O10	0.635(2)	0.492(2)	0.0294(8)	1.6(2)
O11	0.732(2)	0.181(2)	0.0211(7)	1.0(2)
O12	0.405(2)	0.286(2)	−0.0153(6)	0.9(2)
H6	0.342	−0.120	−0.320	3.9
H7	−0.181	0.359	0.228	3.9

Note. $B_{eq} = 8\pi^2/3 \times$ trace u (u diagonalized matrix).

[a] Refined anisotropically.

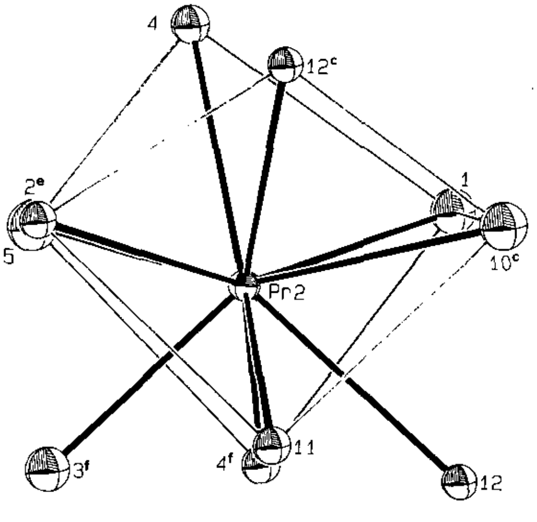

FIG. 2. Coordination polyhedron of Pr2 in $Pr_2(HSeO_3)_2(SeO_3)_2$.

TABLE 3
Selected Distances (Å) and Angles (°) for $Pr_2(HSeO_3)_2(SeO_3)_2$

Pr environment					
Pr1–O1	2.49(1)	Pr2–O1	2.49(1)		
Pr1–O2	2.70(1)	Pr2–O2^e	2.50(1)		
Pr1–O2^a	2.62(1)	Pr2–O3^f	2.48(1)		
Pr1–O3^a	2.77(1)	Pr2–O4	2.60(1)		
Pr1–O8	2.54(1)	Pr2–O4^f	2.47(1)		
Pr1–O8^b	2.47(1)	Pr2–O5	2.68(1)		
Pr1–O9	2.68(1)	Pr2–O10^c	2.74(1)		
Pr1–O10^c	2.49(1)	Pr2–O11	2.55(1)		
Pr1–O11^d	2.50(1)	Pr2–O12	2.69(1)		
Pr1–O12	2.53(1)	Pr2–O12^c	2.62(1)		
⟨Pr1–O⟩	2.58(1)	⟨Pr2–O⟩	2.58(1)		
Se environment					
Se1–O1	1.71(1)	O1–O2	2.59(2)	O1–Se1–O2	93.6(6)
Se1–O2	1.77(1)	O1–O3	2.67(2)	O1–Se1–O3	104.9(7)
Se1–O3	1.67(1)	O2–O3	2.52(2)	O2–Se1–O3	93.9(6)
⟨Se1–O⟩	1.72(1)	⟨O–O⟩	2.59(2)	⟨O–Se1–O⟩	98.4(7)
Se2–O4	1.67(1)	O4–O5	2.49(2)	O4–Se2–O6	95.8(7)
Se2–O5	1.68(2)	O4–O6	2.65(2)	O4–Se2–O6	101.4(8)
Se2–O6	1.75(2)	O5–O6	2.53(2)	O5–Se2–O6	94.7(8)
⟨Se2–O⟩	1.70(2)	⟨O–O⟩	2.55(2)	⟨O–Se2–O⟩	97.3(8)
Se3–O7	1.79(1)	O7–O8	2.66(2)	O7–Se3–O8	102.2(6)
Se3–O8	1.62(1)	O7–O9	2.64(2)	O7–Se3–O9	99.4(7)
Se3–O9	1.67(1)	O8–O9	2.50(2)	O8–Se3–O9	99.0(7)
⟨Se3–O⟩	1.69(1)	⟨O–O⟩	2.60(2)	⟨O–Se3–O⟩	100.2(7)
Se4–O10	1.67(2)	O10–O11	2.69(2)	O10–Se3–O11	107.0(7)
Se4–O11	1.68(1)	O10–O12	2.51(2)	O10–Se3–O12	96.2(7)
Se4–O12	1.71(2)	O11–O12	2.56(2)	O11–Se3–O12	98.4(6)
⟨Se4–O⟩	1.68(1)	⟨O–O⟩	2.59(2)	⟨O–Se–O⟩	100.5(7)
Hydrogen bonding and van der Waals interactions					
O6–H6	0.96(2)	O6–O7^i	2.66(2)	O6–H6–O7^i	111(1)
O7–H7	0.97(1)	O7–O5^g	2.53(2)	O7–H7–O5^g	134(1)
O1–O10^c	2.73(2)	O3–O3^a	2.65(2)		
O2–O8^b	2.67(2)	O2–O12^b	2.68(2)		
O3–O11^c	2.79(2)	O4–O12^c	2.72(2)		
O10–O12^f	2.61(2)				
Interactions between metallic centers					
Pr1–Pr2^d	3.979(1)	Pr1–Pr2	3.999(1)		
Pr1–Pr1^{a,b}	4.3330(6)	Pr2–Pr2^{c,f}	4.3363(6)		

$a = -x, 1/2 + y, z$; $b = -x, y - 1/2, z$; $c = 1 - x, y - 1/2, z$; $d = x-1, y, z$; $e = 1 + x, y, z$; $f = 1 - x, 1/2 + y, z$; $g = x - 1, 1/2 - y, 1/2 + z$; $h = -x, -y, 1/2 + z$; $i = -x, -y; z - 1/2$.

Pr atoms, via selenite groups, two crystallographically equivalents and three independents.

The four selenium atoms are coordinated to three oxygens, forming the classical coordination polyhedron of the Se(IV) trigonal pyramid, which can be considered as a tetrahedron constituted by the three oxygen atoms and the lone pair of electrons (E) occupying an apex. The mean Se–O distance varies from 1.68 Å for Se4 to 1.72 Å for Se1, while the mean O–O distances are of about 2.59 Å (Table 3). Se atoms are not grouped together but they play an important and original role in the building of this structure. In fact, the selenite groups (Se1, Se4) bridge equivalent and inequivalent Pr atoms; e.g., Se1 is bonded to two Pr1 via common O1O2 and O2O3 edges (bischelation), giving rise to a corrugated chain parallel to the [010] axis, previously described. Besides, all the corners of the Se1 atoms are also coordinated to Pr2 atoms (monodentately) (Fig. 3). On the other hand, Se4 plays the same role as Se1 toward Pr2, but in relation to Pr1 atoms. These selenite groups are related to five metallic centers.

A different behavior is exhibited by the hydrogenselenite groups –Se2 and Se3–, which are bonded only to Pr2 and Pr1, respectively, via a common edge (monochelation), but one oxygen of these edges is linked to a supplementary equivalent Pr atom; e.g., for Se3, the O8O9 edge is shared with the Pr1 atom and O8 is coordinated with another Pr1 atom, (Fig. 4). In this way Se2 and Se3, like Se1 and Se4, contribute to the stability of the layers. The hydroxyl groups (O6 for Se2, O7 for Se3) form two bridges between the bidimensional sheets, via two hydrogen bonds, O6–H6 ... O7 and O7–H7 ... O5, along the [001] direction (Fig. 4). These interactions keep the stability of the three-dimensional framework of the structure.

Another feature in this structure deserving mention it is the number of metallic centers, including Se atoms, around each oxygen atom. Apart from the hydroxyl groups (O6, O7), O5 and O9 are μ_2, O1, O3, O4, O8, O10, and O11 are μ_3, and O2 and O12 are μ_4. In the

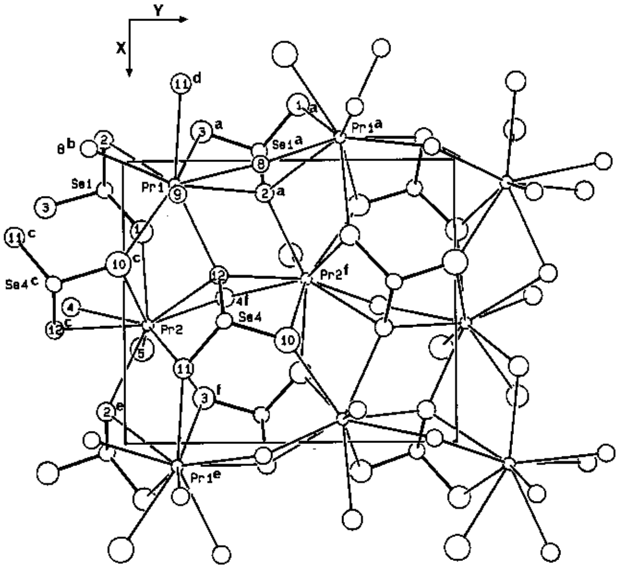

FIG. 3. Representation of the (001) plane of the layers in $Pr_2(HSeO_3)_2(SeO_3)_2$.

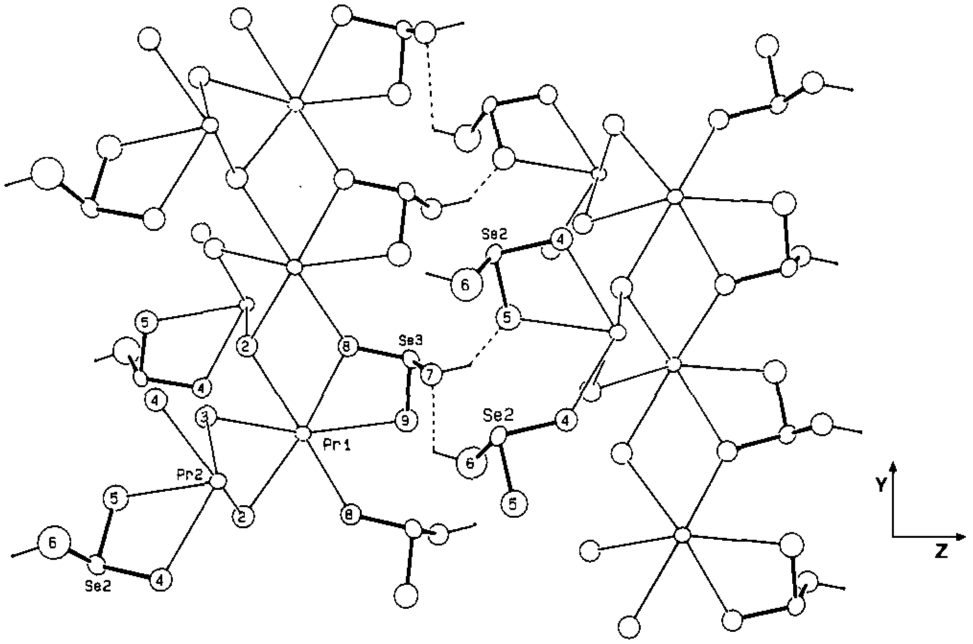

FIG. 4. View of the (100) plane of two layers showing evidence of hydrogen bonding between them.

latter case, the respective angle values around these oxygen atoms do not differ much from that of the tetrahedron, from 96.6 to 124.9° for O2 and from 98.2 to 123.8° for O12.

CONCLUSIONS

The most exciting feature found in the crystal structure of $Pr_2(HSeO_3)_2(SeO_3)_2$ is the existence of simultaneously tri-monodentate and bi-bidentate selenite groups (Se1 and Se4) which bridge five metallic centers (Fig. 3), giving rise to relatively small Pr–Pr distances, as is reported in Table 3. This fact opens the possibility of finding interesting magnetic properties (antiferromagnetic coupling), so a more accurate study of the magnetic behavior of this compound is now in progress.

On the other hand, the knowledge of the crystal structure of $Pr_2(HSeO_3)_2(SeO_3)_2$ allows an understanding of the thermal behavior of this material and a proposed mechanism of decomposition, together with a structural framework for some anhydrous rare-earth selenites, previously reported as microcrystalline powders (9).

In fact, $Pr_2Se_4O_{11}$ is obtained by the total loss of water in $Pr_2(HSeO_3)_2(SeO_3)$; these H_2O molecules arise from hydrogenselenite groups and could give rise to the formation of diselenite groups. This new compound would be formulated as $Pr_2(Se_2O_5)(SeO_3)_2$ and would show a three-dimensional character, in contrast with the bidimensional network of its precursor. In this way, $Pr_2Se_3O_9$, obtained by the loss of one SeO_2 molecule from the above compound, would be formulated as $Pr_2(SeO_3)_3$. A similar behavior is expected for the isostructural phases $Nd_2Se_4O_{11}$ and $Nd_2Se_3O_9$, respectively, isolated in the thermal decomposition of the recently reported $Nd(HSeO_3)(SeO_3) \cdot 2H_2O$ (8). All these facts will be verified by the crystal structure determination, in progress, of single crystals of these anhydrous praseodymium selenites.

ACKNOWLEDGMENTS

The authors express their gratitude to CNRS of France and CSIC of Spain for the aid under the International Scientific Cooperation Program (PICS). A.C. and M.P. thank DGICYT of Spain for its financial support (Project PB92-1088).

REFERENCES

1. J. Galy, G. Meunier, S. Andersson, and A. Åström, *J. Solid State Chem.* **13,** 142 (1975).
2. J. Galy and R. Enjalbert, *J. Solid State Chem.* **44,** 1 (1982).
3. A. Castro, R. Enjalbert, D. Lloyd, I. Rasines, and J. Galy, *J. Solid State Chem.* **85,** 100 (1990).
4. J. A. Alonso, A. Castro, R. Enjalbert, J. Galy, and I. Rasines, *J. Chem. Soc. Dalton Trans.*, 2551 (1992).
5. R. Morris, W. T. A. Harrison, G. D. Stucky, and A. K. Cheetham, *Acta Crystallogr. Sect. C* **48,** 1182 (1992).
6. M. Koskenlinna and J. Valkonen, *Acta Chem. Scand. A* **31,** 457 (1977).
7. E. Immonen, M. Koskenlinna, L. Niinisto, and P. Pakkenen, *Fin. Chem. Lett.*, 67 (1976).
8. M. de Pedro, R. Enjalbert, A. Castro, J. C. Trombe, and J. Galy, *J. Solid State Chem.* **108,** 87 (1994).
9. A. Castro, M. de Pedro, and I. Rasines, *J. Thermal Anal.* **40,** 1109 (1993).
10. M. de Pedro, I. Rasines, and A. Castro, *J. Mater. Sci. Lett.* **12,** 1637 (1993).
11. J. C. Trombe, private communication.

12. A. C. T. North, D. C. Phillips, and F. S. Matthews, *Acta Crystallogr. Sect. A* **24,** 351 (1968).
13. D. T. Cromer and D. Liberman, "International Tables for X-ray Crystallography," Vol. IV. Kynoch, Birmingham, 1974.
14. D. J. Watkin, J. R. Carruthers, and P. W. Betteridge, "Crystal Users Guide." Chemical Crystallography Laboratory, University of Oxford, 1985.
15. C. K. Johnson, "Ortep II Report ORNL 5138." Oak Ridge National Laboratory, Oak Ridge, TN, 1976.
16. L. Niinisto and M. Leskela, "Handbook on the Physics and Chemistry of Rare Earths" (K. A. Gschneider, Jr., and L. Eyring, (Eds.), pp. 91–320. Amsterdam/New York, 1987.
17. Z. Micka, M. Cermak, and D. Niznansky, *Collect. Czech. Chem. Commun.* **55,** 2441 (1990)